

Public Mis-Notification of Coastal Water Quality: A Probabilistic Evaluation of Posting Errors at Huntington Beach, California

JOON HA KIM AND STANLEY B. GRANT*

Department of Chemical Engineering and Materials Science,
The Henry Samueli School of Engineering,
University of California, Irvine, California 92697

Whenever measurements of fecal pollution in coastal bathing waters reach levels that might pose a significant health risk, warning signs are posted on public beaches in California. Analysis of historical shoreline monitoring data from Huntington Beach, southern California, reveals that protocols used to decide whether to post a sign are prone to error. Errors in public notification (referred to here as posting errors) originate from the variable character of pollutant concentrations in the ocean, the relatively infrequent sampling schedule adopted by most monitoring programs (daily to weekly), and the intrinsic error associated with binary advisories in which the public is either warned or not. In this paper, we derive a probabilistic framework for estimating posting error rates, which at Huntington Beach range from 0 to 41%, and show that relatively high sample-to-sample correlations (>0.4) are required to significantly reduce binary advisory posting errors. Public mis-notification of coastal water quality can be reduced by utilizing probabilistic approaches for predicting current coastal water quality, and adopting analog, instead of binary, warning systems.

Introduction

Many government-sponsored environmental monitoring programs issue health advisories whenever pollutant concentrations reach levels that might pose a threat to human health. The utility of health advisory programs logically depends on their ability to disseminate timely and accurate information, in a format that is useful and easy to understand. This study examines the health advisory component of a large (statewide) shoreline water quality monitoring program in California. Health advisories take the form of warning signs that are posted at public beaches whenever shoreline water quality (as measured by fecal indicator bacteria) fails to meet one or more of seven different state standards. The California health advisory program is one of a growing number of such programs nationwide, sponsored in part by the Federal Beaches Environmental and Coastal Health Act passed by the U.S. Congress in October 2000 (1–4). A noteworthy aspect of the California program is its binary nature, in which information about coastal water quality is conveyed to the public by the presence or absence of warning signs on the beach during the high-use period from April 1 through

October 31 of every year. This binary approach stands in contrast to other long-standing reporting programs, for example, weather forecasts, in which the information provided to the public is probabilistic in nature (5).

In this paper, we set out to answer several questions: (1) What is the magnitude of error associated with binary health advisories? (2) How are these error rates affected by the degree to which the concentrations of bacteria in consecutive samples are correlated? (3) Can the accuracy and effectiveness of health advisories be improved by changing the way data are collected and analyzed and/or by changing the way water quality information is conveyed to the public? To answer these questions, we develop a probabilistic framework for analyzing posting errors and compare the theory to observations of posting errors at Huntington Beach in southern California. Huntington Beach is an ideal natural laboratory to examine shoreline water quality issues because of the magnitude of the historical water quality problem, the wealth of available shoreline monitoring data, and the fact that a series of special studies have been conducted with a wide range of sampling frequencies (6–8).

Public Notification of Shoreline Water Quality in California

Beginning July 1, 1999, the State of California mandated fecal indicator bacteria monitoring at all public beaches with more than 50 000 annual visitors and established seven statewide concentration standards for fecal indicator bacteria in the surf zone. When the concentration of indicator bacteria at a monitoring site exceeds any of the California standards, the local health official must post a sign warning beach goers of potential health risks associated with entering the water (*surf zone posting*). If a sewage spill is suspected, the local health official may close the surf to public access (*surf zone closure*). Four of the seven standards are single-sample standards, for which a monitoring site is considered to be out of compliance if the concentration of indicator bacteria in a single sample exceeds specified concentrations for total coliform (TC), fecal coliform (FC), and *Enterococcus* species (ENT). The California single-sample standards for TC, FC, and ENT are respectively 10 000, 400, and 104 most probable number (MPN) or colony forming units (cfu)/100 mL; a fourth single-sample standard for TC of 1000 MPN or cfu/100 mL applies when the TC/FC ratio falls below 10. The remaining standards are 30-day geometric mean standards, for which a monitoring site is considered to be out of compliance if the geometric means of TC, FC, and ENT in all samples collected within a 30-day period exceed 1000, 200, and 35 MPN or cfu/100 mL, respectively. These standards correspond, at least theoretically, to a threshold rate of bather illness of 19 cases of highly credible gastrointestinal disease for every 1000 bathers. (3, 9–11) There are many historical reasons for choosing this particular threshold, including the fact that it represents the background rate of gastrointestinal illness among the general population (12).

Observations of Posting Errors at Huntington Beach

The surf zone posting protocols described above were adopted with the goal of conveying to the public up-to-date information about surf zone water quality. However, a post de facto comparison of posting records and water quality test results indicates that the public is often mis-notified about current water quality conditions. This point is illustrated in Figure 1A where we compare measurements of

* Corresponding author e-mail: sbgrant@uci.edu; phone: (949)824-7320; fax: (949)824-2541.

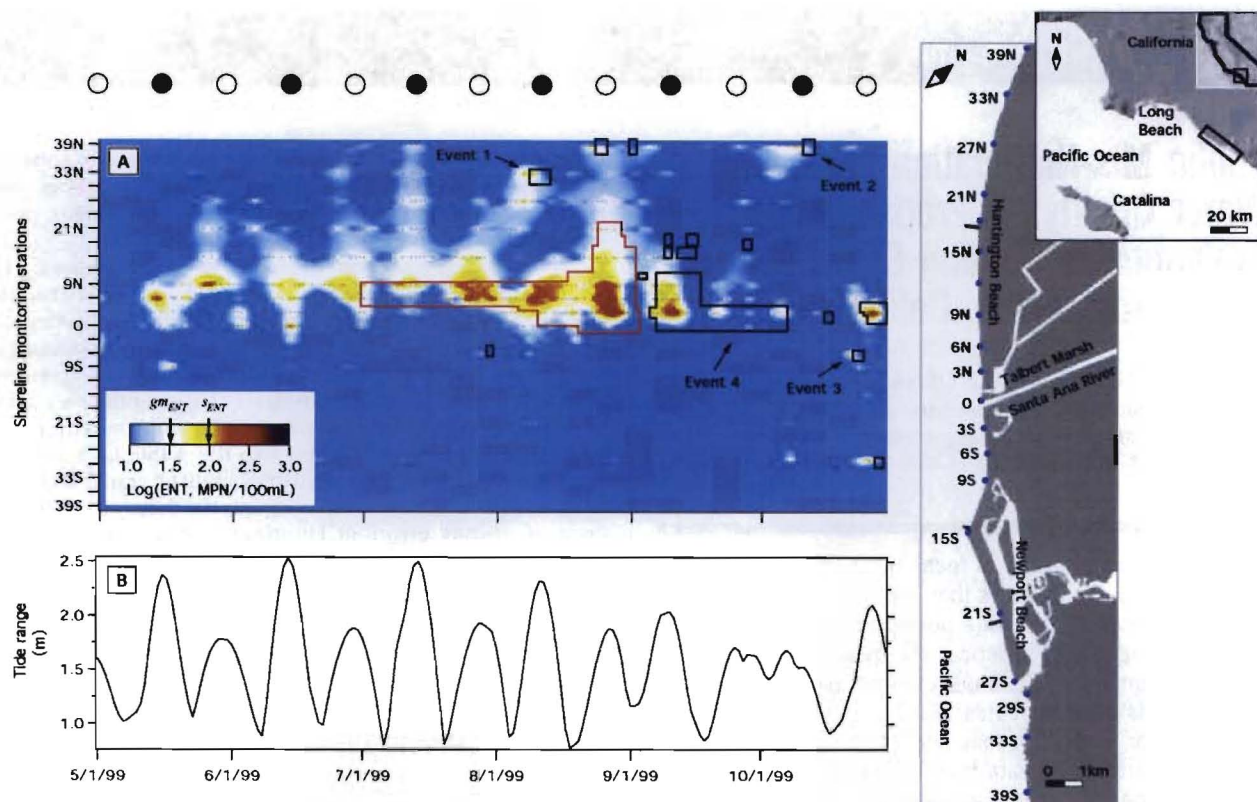


FIGURE 1. (A) Log-transformed concentration of ENT in the surf zone at Huntington Beach and Newport Beach plotted against surf zone stations (vertical axis, see also map) and time (horizontal axis). Each sample collected from the surf zone appears as a small dot in the plot. Open and closed circles at the top of the figure indicate the timing of full and new moons, respectively. Black and red polygons represent the posting and closure history, respectively. gm_{ENT} and s_{ENT} refer to the California geometric mean and single-sample standards for ENT in the surf zone. Several posting events (labeled 1–4) are discussed in the text. **(B)** Plot of the maximum daily tide range, defined as the difference between the daily higher-high and lower-low tides.

ENT in the surf zone at Huntington Beach (color ranging from blue to black) with the posting and closure history (black and red polygons, respectively) over the period May 1–October 31, 1999. This time period was selected because it includes the summer of 1999 when Huntington Beach experienced a record number of postings and closures, and it straddles the start of California's new water quality regulations that went into effect July 1, 1999. Most (95%) of the postings indicated in the figure were triggered by the single-sample and geometric mean standards for ENT. Yet there are many instances when the concentration of ENT exceeded the single-sample standard but signs were not posted (referred to here as underprotection errors) or where the concentration of ENT was below the single-sample standard but signs were posted (overprotection errors). Often, overprotection errors immediately follow underprotection errors (e.g., see events 1–3 in Figure 1A). Presumably, posting errors caused by the single-sample standards originate from the variable nature of water quality in the surf zone (see next section) and the inherent time delay (ca. 2–3 d) between when a sample is collected and when a sign is posted or taken down. The geometric mean standard also triggered overprotection errors involving multiple shoreline stations and lasting several weeks (see last half of event 4 in Figure 1A). The geometric mean is computed from test results collected at a particular site over the preceding 30 days (the so-called 30-day geometric mean standard); therefore, once a violation has occurred, a relatively large sequence of compliant samples are required before the geometric mean falls back below the standard. It should also be noted that the use of geometric means for evaluating human health risk has been challenged on theoretical grounds (13).

Importantly, we note that beach *closures* can be more accurate predictors of poor water quality than beach *postings*. Beginning on July 1, 1999, the local health officer closed sections of Huntington Beach out of concern that the surf zone contamination might be from a source of sewage (red polygon in Figure 1A). From personal observations, the health officer was aware that the concentration of fecal indicator bacteria in the surf zone at Huntington Beach was generally highest during full and new moons (when the daily tide range is maximal, compare Figure 1, panels A and B) (14). Awareness of these lunar cycles influenced the health officer's decisions about when to close the beach and was one of the factors that allowed him to correctly anticipate the large pollution event that occurred during the full moon in early September (see large closure event in Figure 1A). This anecdote suggests that posting error rates might be reduced if posting protocols were designed to take into account factors known, through past experience, to influence local water quality. Some of the factors affecting surf zone water quality are described next.

Patterns and Randomness in Shoreline Water Quality

Surf zone water quality has both periodic patterns and random fluctuations. The concentration of fecal indicator bacteria in the surf zone at Huntington Beach, for example, exhibits a cascade of periodic patterns including (6–8): (1) tidal cycling in which the concentration is higher during ebb tides and lower during flood tides (or vice versa); (2) diurnal cycling in which the concentration is higher at night and lower during the day; (3) spring–neap cycling in which the concentration is higher during spring tides and lower during neap tides (evident in Figure 1A); (4) seasonal cycling in which the concentration is higher during the winter storm season and lower during the summer dry season; (5) El Niño cycling

in which the concentration is higher during stormy El Niño winters and lower during dry La Niña winters; (6) multi-decadal patterns in which periodic large-scale investment in sewage and storm runoff infrastructure improves coastal water quality.

Monitoring programs can detect these periodic patterns only if the time interval between samples is smaller (by at least a factor of 2) as compared to the characteristic period of a particular pattern of interest (15). For example, samples must be collected at least every 3 h in order to detect tidal cycling because each ebb and flood tide lasts ca. 6 h. Routine monitoring programs in California, which typically sample each site once per day to once per week, can detect patterns 3–6 described above depending on the length of time over which data are available. Importantly, processes with characteristic periods less than the sampling interval cannot be detected because the water quality signal is aliased by the sampling program. The relative uncertainty associated with the water quality sampling and testing methods, which ranges up to 23% (16), is also a source of noise (17). In the next several sections, we develop and test a probabilistic model that can account for the repeating patterns and random noise inherent in water quality measurements. To make the results of the probabilistic analysis accessible to a broad audience, each section begins with the primary question to be addressed, immediately followed by the answer supported by the analysis.

Probability of Single-Sample Exceedences

Question: Can the fraction of samples violating single-sample standards be predicted from statistical features of local water quality, such as measures of central tendency and spread?

Answer: The fraction of samples violating single-sample standards can be predicted from the log-mean and standard deviation of fecal indicator monitoring data, provided that the data are well described by a log-normal distribution. Furthermore, the theory predicts and observations confirm that, under certain conditions, a marginal change in water quality can lead to a substantial change in the number of signs posted at the beach.

The probability that the concentration of bacteria in a single sample will exceed a standard (s) can be represented mathematically as follows:

$$P_{\text{ex}} = P[C > s] = \int_s^{\infty} f_C(c) dc \quad (1)$$

where C is a random concentration variable, c is a particular realization of the random variable, and $f_C(c)$ is the probability density function for the concentration of fecal indicator bacteria in the surf zone. The exceedence probability (P_{ex}) is a measure of water quality: $P_{\text{ex}} \rightarrow 1$ if water quality is very poor, and $P_{\text{ex}} \rightarrow 0$ if water quality is very good.

The monitoring data at Huntington Beach conform reasonably to a log-normal distribution (based on Kolmogorov–Smirnov normality tests (18); maximum difference $K - S = 0.08$ at the significant level $\alpha < 0.01$) (see Figure S1 in the Supporting Information) as do monitoring data at other coastal sites throughout the world (19–21). Accordingly, we replaced C with $\log C$ in eq 1 and substituted the Gaussian probability distribution function for $f_{\log C}(\log c)$. After simplification, the following relationship was obtained between the exceedence probability and a nondimensional variable referred to here as S^* :

$$P_{\text{ex}} = \frac{1}{2} \text{erfc } S^* \quad (2a)$$

$$S^* \equiv \frac{\log s - \mu_{\log C}}{\sqrt{2}\sigma_{\log C}} \quad (2b)$$

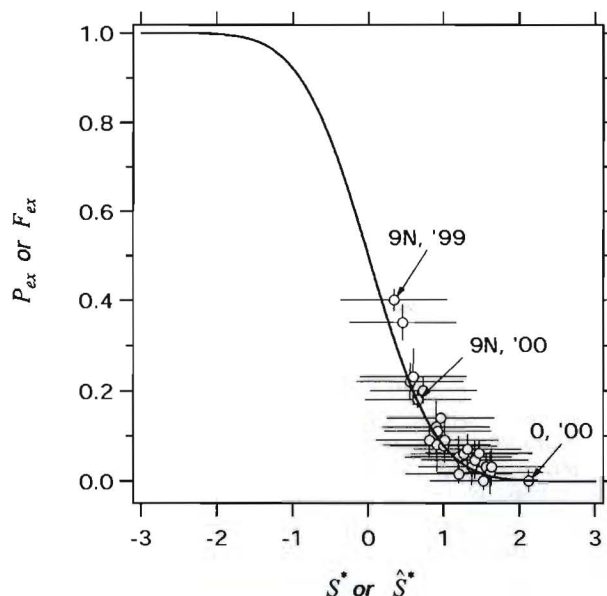


FIGURE 2. Predicted relationship between the probability P_{ex} that samples will exceed a single-sample standard and the dimensionless parameter S^* (solid line, eq 2a). Data points represent observed relationship between the fraction F_{ex} of samples collected at Huntington Beach that exceeded the single-sample standard for ENT plotted against the parameter \hat{S}^* . The vertical and horizontal error bars correspond to $\pm\sqrt{F_{\text{ex}}(1-F_{\text{ex}})/n}$ and $\pm 1/\sqrt{2}$, respectively, where n is the number of data points in each data bin ($n = 45-65$)

In these equations, erfc is the complementary error function, and $\mu_{\log C}$ and $\sigma_{\log C}$ represent the mean and standard deviation of the log-transformed bacterial concentrations, respectively. This simple theoretical result predicts that the exceedence probability decreases with increasing values of the parameter S^* , ranging from $P_{\text{ex}} > 99\%$ when $S^* < -2$ to $P_{\text{ex}} < 1\%$ when $S^* > 2$ (solid line in Figure 2). In turn, the value of S^* depends on local water quality ($\mu_{\log C}$ and $\sigma_{\log C}$) and the magnitude of the single-sample standard ($\log s$).

These theoretical predictions compare well with observations of single-sample exceedences at Huntington Beach. To compute the latter, summertime measurements of ENT in the surf zone at Huntington Beach were grouped, or binned, by station and year. For example, one bin constituted all ENT measurements collected at surf zone station 9N during the summer of 1999; for the purposes of this analysis, summer is defined as the time period June 1–August 31. From each data bin, we calculated the fraction F_{ex} of samples that violated the single-sample standard for ENT and an empirical approximation of the parameter S^* denoted here as \hat{S}^* (see Supporting Information, note that the circumflex or “hat” denotes empirical approximations of population parameters). Values of F_{ex} and \hat{S}^* track the theoretical prediction closely (compare solid line with data points in Figure 2); hence, eq 2a appears to capture the relationship between measured water quality ($\hat{\mu}_{\log C}$ and $\hat{\sigma}_{\log C}$) and the fraction of samples that exceed a single-sample standard (F_{ex}). At Huntington Beach, the percentage of samples exceeding the single-sample standard for ENT ranges from a low of 0% ($F_{\text{ex}} = 0$) at surf zone station 0 during the summer of 2000 to a high of 40% ($F_{\text{ex}} = 0.4$) at station 9N during the summer of 1999 (see arrows in Figure 2).

From the shape of the theoretical curve in Figure 2, a marginal change in water quality can result in a very large or a very small change in the number of signs posted at the beach, depending on the absolute magnitude of the parameter S^* . In particular, eq 2a predicts that P_{ex} is sensitive to marginal changes in water quality when $|S^*| < 1$ and

insensitive to marginal changes in water quality when $|S^*| > 1$. This observation helps to explain why the number of signs posted during the summer at 9N decreased precipitously from 26 in 1999 to 12 in 2000, despite the relatively small change in the log-mean of ENT over these two summers (1.7–1.4 units of $\log(\text{MPN}/100 \text{ mL})$) (see two arrows in Figure 2).

Probability of Binary Advisory Posting Errors

Question: How is the posting error rate influenced by the degree to which bacterial concentrations in consecutive samples are correlated? At Huntington Beach, are bacterial concentrations in consecutive samples correlated or independent realizations?

Answer: Theory predicts very high posting error rates when S^* is close to zero, even in the case where the concentrations of fecal indicator bacteria in consecutive samples are moderately correlated. This prediction is borne out by an analysis of ENT measurements in the surf zone at Huntington Beach. Posting error rates at Huntington Beach are indistinguishable from the predictions of Bernoulli trial theory, which is premised on the idea that test outcomes are independent realizations. When S^* is close to zero, posting error rates are predicted to range from 35% (for moderately correlated samples) to 50% (for weakly correlated samples).

Let $\alpha(t_i)$ represent the measured concentration of fecal indicator bacteria at a particular site at time t_i . The single-sample standard posting protocol can be stated succinctly as follows. A water sample is collected at a particular site at time t_{i-1} , and the concentration of fecal indicator bacteria in that sample $\alpha(t_{i-1})$ is compared to a single-sample standard s . If $\alpha(t_{i-1}) > s$, a sign is posted at the site; if $\alpha(t_{i-1}) < s$, a sign is not posted at the site (or an existing sign at the site is removed). If t_i denotes the time at which a sign is posted (or removed), four possible outcomes can be identified: (1) $\alpha(t_{i-1}) > s$ and $\alpha(t_i) > s$, (2) $\alpha(t_{i-1}) < s$ and $\alpha(t_i) < s$, (3) $\alpha(t_{i-1}) < s$ and $\alpha(t_i) > s$, and (4) $\alpha(t_{i-1}) > s$ and $\alpha(t_i) < s$. No error occurs in cases 1 and 2 because the public has been correctly informed that water quality exceeds standards (case 1) or does not exceed standards (case 2). Posting error occurs when the public is incorrectly informed that water quality meets standards (case 3), or incorrectly informed that water quality does not meet standards (case 4). Consistent with the discussion of Figure 1A (see above), we refer to cases 3 and 4 as underprotection and overprotection posting errors, respectively.

Letting the superscripts U, O, and T represent underprotection, overprotection, and total posting error (defined as the sum of underprotection and overprotection errors), the following expressions can be derived for the probability that posting errors will occur at a particular site (see Supporting Information):

$$P_{\text{err}}^{\text{U}} = P_{\text{err}}^{\text{O}} = \frac{1}{2} \text{erfc } S^* \left[1 - \frac{1}{2} \text{erfc } S^* G(S^*, \rho(1)) \right] \quad (3a)$$

$$P_{\text{err}}^{\text{T}} = \text{erfc } S^* \left[1 - \frac{1}{2} \text{erfc } S^* G(S^*, \rho(1)) \right] \quad (3b)$$

The function $G(S^*, \rho(1))$ depends on the value of S^* and $\rho(1)$, where S^* has been defined previously (see eq 2b) and $\rho(1)$ is the correlation coefficient between fecal indicator bacteria concentrations at times t_{i-1} and t_i . A mathematical definition and graphical representation of $G(S^*, \rho(1))$ is included with the Supporting Information (Figure S2). The total posting error predicted by eq 3b is plotted against S^* in Figure 3. The different lines in the figure correspond to different choices of the correlation coefficient $\rho(1)$, ranging from strong positive correlation ($\rho(1) = 0.95$) to strong negative correlation ($\rho(1) = -0.95$). For the choice of $\rho(1)$

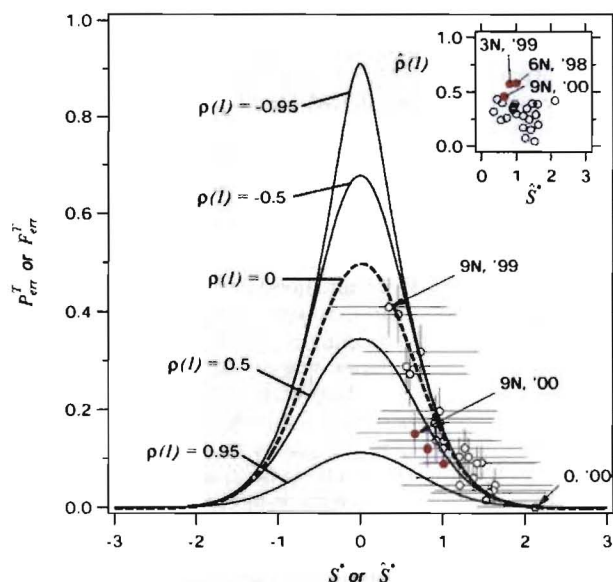


FIGURE 3. Predicted relationship between the probability of a posting error $P_{\text{err}}^{\text{T}}$ and the dimensionless parameter S^* (solid and dashed curves, eq 3b). The different curves correspond to different choices of the correlation coefficient $\rho(1)$. Points represent posting error rates calculated from the surf zone monitoring data at Huntington Beach. Vertical and horizontal error bars correspond to $\pm F_{\text{err}}^{\text{T}} \sqrt{F_{\text{err}}^{\text{T}}(1-F_{\text{err}}^{\text{T}})/n}$ and $\pm 1/\sqrt{2}$, respectively, where n represents the number of points in a particular data bin (see text). Inset is a plot of the correlation coefficient between bacterial concentrations in consecutive samples $\hat{\rho}(1)$ against the parameter \hat{S}^* . The red points correspond to surf zone stations and years where the posting error rate fell substantially below the error rate predicted by Bernoulli trial theory ($\rho(1) = 0$).

$= 0$, the concentrations of bacteria in consecutive samples are completely uncorrelated (i.e., every concentration measurement is independent of the one before it), and the function $G(S^*, \rho(1))$ reduces to unity for all choices of S^* . In this limit, referred to here as the Bernoulli trial theory limit, the probability of an overprotective or underprotective posting error peaks at $P_{\text{err}}^{\text{T}} = 0.5$ when $S^* = 0$ (dashed line in Figure 3). Put another way, when the concentrations of bacteria in consecutive samples are uncorrelated ($\rho(1) = 0$) and half of samples exceed the single-sample standard ($S^* = 0$, $P_{\text{ex}} = 0.5$), theory predicts that beach signage will be posted (or not posted) in error 50% of the time ($P_{\text{err}}^{\text{T}} = 0.5$).

The peak error rate, which always occurs at $S^* = 0$, decreases with increasing $\rho(1)$, approaching zero (i.e., no error) in the limit where the concentrations of bacteria in consecutive samples are perfectly correlated ($\rho(1) = 1$) (Figure 3). In the event that concentrations of bacteria in consecutive samples are negatively correlated ($\rho(1) < 0$), the peak error rate exceeds 50%, approaching 100% in the extreme limit where $\rho(1) = -1$. Even in cases where the concentrations of bacteria in consecutive samples are reasonably well-correlated, say $\rho(1) = 0.5$, relatively large peak posting error rates are predicted ($P_{\text{err}}^{\text{T}} = 0.35$).

To test the theory presented above, the fraction $F_{\text{err}}^{\text{T}}$ of samples that generated underprotection or overprotection posting errors was calculated for each of the Huntington Beach data bins described in the last section (see Supporting Information). Values of $F_{\text{err}}^{\text{T}}$ track closely the theoretical line for $\rho(1) = 0$ (i.e., the Bernoulli trial theory limit, compare data points with dashed line in Figure 3), consistent with the idea that the concentrations of ENT in consecutive samples at Huntington Beach are uncorrelated. To explore this issue further, for each data bin, we calculated the correlation coefficient between ENT concentrations in consecutive

samples, referred to here as $\hat{\rho}(1)$ (see inset in Figure 3). Empirical correlation coefficients range from $\hat{\rho}(1) = 0.04$ to 0.58; averaging across all bins, we obtain $\overline{\hat{\rho}(1)} = 0.32 \pm 0.13$. The concentration of ENT in consecutive samples are not completely uncorrelated (i.e., $\hat{\rho}(1) \neq 0$); however, the sample-to-sample correlation is sufficiently weak such that total posting error rates are indistinguishable, within the resolution of our estimates of F_{err}^T , from the predictions of Bernoulli trial theory. An exception may be the three data bins with the highest correlation coefficients: station 6N in 1998, station 3N in 1999, and station 9N in 2000 (compare red points and dashed line in Figure 3).

Can Increasing the Sampling Frequency Reduce Posting Errors?

Question: Would the sample-to-sample correlation be higher and the rate of single-sample posting errors be lower if surf zone samples were collected more frequently?

Answer: An analysis of ENT data at Huntington Beach reveals that posting decisions would have to be updated every 40 min (or more frequently) to significantly reduce posting errors. Even if posting decisions were revised every 10 minutes, when S^* is close to zero as much as 30% of the signage would be in error. This result will likely apply to any shoreline site where the sampling time interval is longer than the persistence time of pollution patches in the surf zone.

The question is motivated by the growing interest in developing rapid fecal indicator bacteria tests that could, in principle, dramatically reduce the time between when a sample is taken and the bacterial indicator concentration is known (22). The answer derives from an analysis of autocorrelation functions computed from four different time series (Figure 4): (1) Routine ENT monitoring data at station 9N, subsampled to yield a sampling frequency of once per week ($\Delta t = 1$ week, panel A). (2) Routine ENT monitoring data at station 9N subsampled to yield a sampling frequency of once per 3 days ($\Delta t = 3$ days, panel B). (3) A special ENT monitoring study at station 3N in which water samples were collected every hour, 24 h per day, for 2 weeks ($\Delta t = 1$ h, panel C). (4) A second special ENT monitoring study at station 6N in which water samples were collected every 10 min for a total of 12 h ($\Delta t = 10$ min, panel D). The autocorrelation functions in Figure 4 represent the correlation $\hat{\rho}(\Delta t_j)$ between a time series and itself after introducing a lag of j points or, equivalently, a time lag of $\Delta t_j = j\Delta t$. For comparison, also plotted in each panel of the figure are autocorrelation functions calculated from a sequence of random numbers ranging in magnitude from 1 to -1 (black lines in each panel).

Correlation $\hat{\rho}(\Delta t_j)$ falls off very rapidly with increasing lag Δt_j for sampling intervals of $\Delta t = 1$ week and 3 d (red curves in panels A and B, respectively). When $\Delta t = 1$ week (panel A), a broad peak is evident at time lags of 40–50 weeks (i.e., approximate 1 yr), presumably due to the influence of seasonal rainfall on bacterial concentrations in the surf zone. Spring–neap cycling of bacterial concentration is apparent in panel B where the correlation values peak every 2 weeks. Apart from the seasonal (panel A) and spring–neap (panel B) patterns, the correlation coefficients calculated for these two cases are generally within the range calculated from a sequence of random numbers (black lines). Correlation peaks are present at multiples of 24 h when the surf zone is sampled every hour ($\Delta t = 1$ h, panel C). This diurnal cycle probably arises from the germicidal affect of sunlight (7), although tidal processes may also play a role (e.g., during the summer at Huntington Beach there is typically just one large ebb tide per day). Remarkably, the sign of $\hat{\rho}(\Delta t_j)$ in Figure 4C is periodically negative, implying that posting error rates might increase if the sampling frequency is increased, for example, from once per day to once every 12 h (see peak error rates

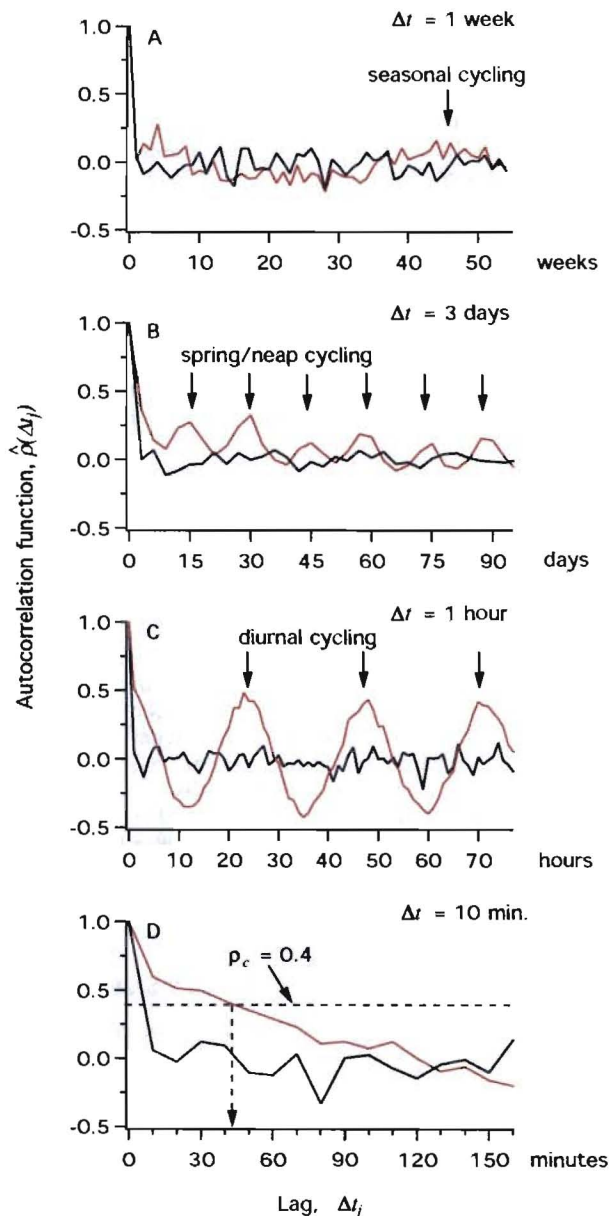


FIGURE 4. Autocorrelation functions calculated from four different time series (red lines in each panel) and from a sequence of uncorrelated (random) numbers (black lines in each panel). The time interval between samples (Δt) is noted in each panel (see text for details). The number of samples used for the analysis in each panel is $n = 216$ (panel A), 528 (panel B), 337 (panel C), and 61 (panel D).

when $\rho(1) < 0$ in Figure 3). Compared to the other autocorrelation functions, $\hat{\rho}(\Delta t_j)$ decays with Δt_j more slowly when samples are collected every 10 min (panel D). Even in this case, however, the correlation coefficient for a lag of 10 min ($\hat{\rho}(\Delta t = 10 \text{ min.}) = 0.6$) is such that substantial posting errors ($\approx 30\%$) are predicted when $S^* \approx 0$ (see Figure 3). Put another way, if the time interval between when a sample is taken and a sign is posted (or removed) was reduced to just 10 min, as much as 30% of the signage could be in error. The technology for rapid detection of fecal indicator bacteria is maturing such that near real-time measurements of these organisms may be feasible soon. Even if bacterial measurements could be carried out instantaneously (i.e., $\Delta t \rightarrow 0$ and $\rho(1) \rightarrow 1$), however, it is not clear how that information would be used in practice. Given the highly variable nature of the coastal water quality signal, health advisories would have to be updated on a minute-by-minute basis, creating an untenable

situation for both local officials who issue health advisories and the beach-going public.

On the basis of the autocorrelation functions presented in Figure 4A,B and the correlation values calculated from ENT monitoring data at Huntington Beach (inset in Figure 3), it appears that $\hat{\rho}(1) \leq 0.4$ is typical of sampling frequencies in the once-per-day to once-per-week range. Because the posting error rates calculated from the daily to weekly monitoring data closely follow the predictions of Bernoulli trial theory (see Figure 3), it seems reasonable to adopt 0.4 as the critical correlation value above which Bernoulli trial theory begins to break down ($\rho_c \approx 0.4$). Referring to Figure 4D, the correlation $\hat{\rho}(\Delta t)$ falls below 0.4 for lag times greater than approximately 40 min (see dashed arrow in figure). This lag is very close to the time it takes tidally generated patches of fecal pollution in the Huntington Beach surf zone to advect past a fixed location by wave-driven long-shore currents ($\tau = L/u = 50$ min, where $L = 1$ km is the approximate length of an average pollution patch and $u = 0.3$ m/s is a typical long-shore advective velocity) (7, 8). Therefore, the concentration of bacteria in a water sample from the surf zone appears to have little memory of previous samples (and hence Bernoulli trial theory applies) so long as the time interval between samples is longer than the persistence time of pollution patches. While the persistence time scale will vary by site, given the highly dynamic nature of ocean currents at most coastal sites it is unlikely that the persistence time scale will exceed 1 d, the sampling frequency of the most aggressive shoreline monitoring programs. Hence, the large posting error rates reported in this paper are probably not unique to Huntington Beach. Rather, large errors can be expected at any marine or freshwater beach when $|S^*| < 1$ and the time interval between samples is greater than the persistence time scale for patches of contaminated water.

Toward an Analog Public Health Advisory System

Question: *Can less error-prone approaches be developed for assessing current water quality and reporting that information to the public?*

Answer: *Several different approaches can be adopted to predict (or "now-cast") current coastal water quality and report that information to the general public. At Huntington Beach, the current concentration of ENT at a particular surf zone station is generally more correlated with the maximum daily tide range, than with the concentration of bacteria in the last sample.*

An approach that follows naturally from the probability theory presented above involves computing analog (i.e., continuously varying) estimates of current water quality and/or human health risk, periodically updated as new information becomes available. Predictions of current water quality, or now-casts, could utilize a variety of data resources including recent water quality test results and real-time (or near-real-time) measurements of quantities known to correlate with local surf zone water quality. Now-casts, in turn, could be conveyed to the public through a combination of web sites, newspaper reports, and/or beach signage either in raw form or using a grading scale like that employed by Heal the Bay (23).

As an example, below we present a prototypical algorithm that now-casts three different measures of water quality. For the sake of simplicity and to demonstrate the power of even a modest algorithm, our prototype requires only estimates of tide range (predicted from WXTide32 (24)) and water quality measurements collected over the previous 30 d. At the heart of the algorithm is the assumption that current water quality is conditioned on maximum daily tide range, as expressed quantitatively through the conditional prob-

ability density function, $f_{\log C|L}(\log c|l)$. Here, $\log C$ and L represent random variables for the log-transformed bacterial concentration and maximum daily tide range, respectively, and $\log c$ and l are specific realizations of the random variables. For a fixed value of the tide range l , the probability of single-sample exceedence and expected value of the bacterial concentration can be calculated as follows:

$$P_{\text{ex}|\ell} \equiv P[\log C > \log s | L = \ell] = \int_{\log s}^{\infty} f_{\log C|L}(x|\ell) dx \quad (4a)$$

$$\mu_{\log C|\ell} \equiv E[\log C | L = \ell] = \int_{-\infty}^{\infty} x f_{\log C|L}(x|\ell) dx \quad (4b)$$

An analysis of maximum daily tide-range predicted for Huntington Beach reveals that L conforms reasonably well to a normal distribution (based on Kolmogorov-Smirnov normality tests; maximum difference $K - S = 0.04$ at the significant level $\alpha < 0.01$) as do the log-transformed concentrations of fecal indicator bacteria (see earlier). This implies that eqs 4a,b can be written explicitly as follows (see Supporting Information):

$$P_{\text{ex}|\ell}(S^*, \ell^*, \rho_{CL}) = \frac{1}{2} \text{erfc}[(S^* - \rho_{CL} \ell^*) / \sqrt{1 - \rho_{CL}^2}] \quad (5a)$$

$$\mu_{\log C|\ell} = \mu_{\log C} + (\rho_{CL} \sigma_{\log C} / \sigma_L)(\ell - \mu_L) \quad (5b)$$

$$\sigma_{\log C|\ell} = \sigma_{\log C} \sqrt{1 - \rho_{CL}^2} \quad (5c)$$

where $\ell^* = (\ell - \mu_L) / (\sqrt{2} \sigma_L)$, ρ_{CL} is the correlation coefficient between $\log C$ and L , μ_L and σ_L are the mean and standard deviation of the maximum daily tide range, and the other parameters have been defined previously. Equation 5b is a linear model for the dependence of $\mu_{\log C|\ell}$ on ℓ , with coefficients equivalent to those obtained by a mean-square regression of $\mu_{\log C|\ell}$ against ℓ (25). To develop an expression for bathery illness rate, we utilized the linear relationship for gastrointestinal illness rate per 1000 bathers (Y) reported by Cabelli et al. (9): $Y = a + b \log GM_C$, where GM_C represents the geometric mean of ENT measurements, and $a = -5.1$ and $b = 24.2$ are empirical constants. Rewriting Cabelli et al.'s model in terms of the conditional log-mean $\mu_{\log C|\ell}$ we obtain:

$$Y = a + b \mu_{\log C|\ell} \quad (6a)$$

$$\sigma_Y = \sqrt{\sigma_a^2 + \sigma_b^2 \mu_{\log C|\ell}^2 + b^2 \sigma_{\log C|\ell}^2} \quad (6b)$$

The estimate of uncertainty in Y (eq 6b) was derived by propagating uncertainties in the variables on the RHS of eq 6a (17). This set of expressions (eqs 5a-c and 6a,b) were employed to now-cast water quality at surf zone station 6N over the period May 1–October 31, 1999 (i.e., the same period of time encompassed by Figure 1A). Now-casts for a particular day were generated using the current day's maximum tide range l (estimated from WXTide32) and updated estimates for $\hat{\mu}_{\log C}$, $\hat{\sigma}_{\log C}$, $\hat{\mu}_L$, $\hat{\sigma}_L$, and $\hat{\rho}_{CL}$ calculated from daily tide range and ENT measurements collected over the previous 30 d (see Supporting Information). Values for $\hat{\sigma}_a = 6.35$ and $\hat{\sigma}_b = 4.15$ were estimated from data reported in Cabelli et al. (9).

Now-casts of the ENT concentration at 6N correctly capture the magnitude and spring-neap cycling of actual ENT measurements (compare red and blue curves, second panel of Figure 5). Over the 6-month period, 56% and 92% of the ENT measurements at 6N fell in the predicted range $\hat{\mu}_{\log C|\ell} \pm 1 \hat{\sigma}_{\log C|\ell}$ (blue band in second panel) and $\pm 2 \hat{\sigma}_{\log C|\ell}$, respectively. Now casts of illness rate (third panel) are generally above the threshold level of 19 in 1000 (dashed

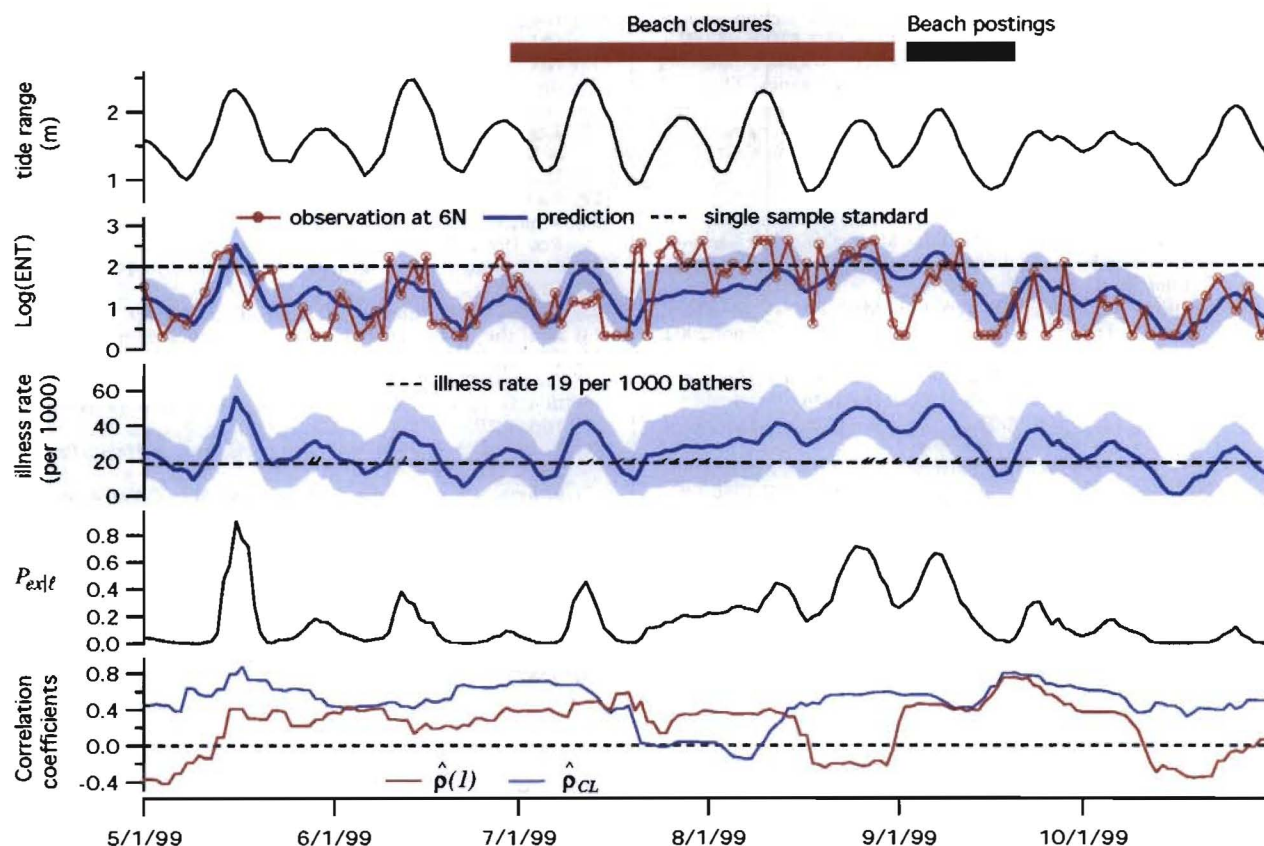


FIGURE 5. Time series plots of maximum daily tide range (top panel), now-casts of ENT concentration (blue line, second panel), illness rates (blue line, third panel), and probability of exceeding the single-sample standard for ENT (black line, fourth panel) at surf zone station 6N in Huntington Beach. Blue bands in second and third panels represent ± 1 SD (see eqs 5c and 6b); red curve in second panel is actual measurements of ENT at 6N. Bottom panel is a plot of the correlation coefficients between ENT in consecutive samples ($\hat{\rho}(1)$) and between ENT and maximum daily tide range ($\hat{\rho}_{CL}$).

horizontal line), peaking at about 60 excess illnesses per 1000 bathers; these illness attack rates are in the range estimated by other researchers for the Huntington Beach area (26). Now-casts for the exceedence probability (fourth panel) exhibit spring–neap cycling, and importantly, periods of high exceedence probability (e.g., $P_{ex|t} > 0.2$) generally coincide with single-sample violations (compare second and fourth panels, Figure 5). The last panel in the figure is a plot of the correlation coefficient between ENT concentrations in consecutive samples ($\hat{\rho}(1)$, red line) and between ENT concentration and maximum daily tide range ($\hat{\rho}_{CL}$, blue line). These two coefficients were updated every day in the 6-month period encompassed by Figure 5, using ENT and maximum daily tide range data collected (ENT) or calculated (tide range) over the previous 30 d. In general, $\hat{\rho}_{CL}$ is larger than 0.4 (i.e., $\hat{\rho}_{CL} > \rho_C$, see earlier) and larger than the correlation between the concentrations of bacteria in consecutive samples ($\hat{\rho}_{CL} \geq \hat{\rho}(1)$). The exception is an approximately 1-month period, centered around August 1, when $\hat{\rho}_{CL} \approx 0$. Not surprisingly, this was also the period when our now-cast model performed least well. In general, at Huntington Beach, the current concentration of bacteria at a particular surf zone station is more correlated with the maximum daily tide range than with the concentration of bacteria in the last sample.

The model presented above could be improved by utilizing all physical variables known through past experience to correlate with coastal water quality and/or by adopting alternative now-casting methodologies (e.g., artificial neural networks (27–29)) that tolerate nonlinear relationships between dependent and independent variables. As mentioned above, the ideal advisory system will be analog in nature; however, even if the current binary approach is

retained, posting decisions based on now-cast methodologies, like the one described here, would be an improvement over the status quo. If the now-casts of ENT presented in Figure 5 had been used as the basis for posting decisions at Huntington Beach during the summer of 1999, for example, the total posting error rate there would have been reduced between 7.5% and 50% (depending on the particular surf zone station of interest).

Acknowledgments

The authors gratefully acknowledge funding from the UC Marine Council (UC Office of the President, 32114); the National Water Research Institute (02-EC-003); and matching funds from the County of Orange, the Santa Ana Regional Water Quality Control Board, and coastal cities in Orange County. J.H.K. was supported by a UC Marine Council fellowship (01-T-CEQI-09-1074). The authors would also like to thank three anonymous reviewers for their critical reviews and the following individuals and institution for feedback: R. Newcomb, S. Ensari, C. McGee, S. Weisberg, B. Sanders, L. Grant, C. Crompton, R. Linsky, R. McCraw, K. Theisen, T. J. Kim, and the California Beach Water Quality Work Group; L. Grant suggested the title.

Supporting Information Available

Mathematical derivations and additional data. This material is available free of charge via the Internet at <http://pubs.acs.org>.

Literature Cited

- (1) Beaches Environmental Assessment and Coastal Health (BEACH) Act of 2000. Public Law 106-284, 2000, pp 870–877.

- (2) *The BEACH Program*; U.S. Environmental Protection Agency, Office of Water: Washington, DC, 1997; EPA-820/F-97-002.
- (3) *Implementation Guidance for Ambient Water Quality for Bacteria*; U.S. Environmental Protection Agency, Office of Water: Washington, DC, 2002; EPA-823/B-02-003.
- (4) *National Beach Guidance and Required Performance Criteria for Grants*; U.S. Environmental Protection Agency, Office of Water: Washington, DC, 2002; EPA-823/B-02-004.
- (5) Palmer, T. N. *Rep. Prog. Phys.* 2000, 63, 71–116.
- (6) Grant, S. B.; Sanders, B. F.; Boehm, A. B.; Redman, J. A.; Kim, J. H.; Mrse, R. D.; Chu, A. K.; Gouldin, M.; McGee, C. D.; Gardiner, N. A.; Jones, B. H.; Svejksky, J.; Leipzig, G. V. *Environ. Sci. Technol.* 2001, 35, 2407–2416.
- (7) Boehm, A. B.; Grant, S. B.; Kim, J. H.; McGee, C. D.; Mowbray, S.; Clark, C.; Foley, D.; Wellmann, D. *Environ. Sci. Technol.* 2002, 36, 3885–3892.
- (8) Kim, J. H.; Grant, S. B.; McGee, C. D.; Sanders, B. F.; Largier, J. L. *Environ. Sci. Technol.* 2004, 38, 2626–2636.
- (9) Cabelli, V. J.; Dufour, A. P.; McCave, L. J.; Levin, M. A. *Am. J. Epidemiology* 1982, 115, 606–616.
- (10) *Ambient Water Quality for Bacteria—1986*; U.S. Environmental Protection Agency, Office of Water: Washington, DC, 1986; EPA-440/5-84-002.
- (11) *Implementation Guidance for Ambient Water Quality for Bacteria—1986*; U.S. Environmental Protection Agency, Office of Water: Washington, DC, 2000; EPA-823/D-00-001.
- (12) Pruss, A. *Int. J. Epidemiol.* 1998, 27, 1–9.
- (13) Haas, C. N. *Water Res.* 1996, 30, 1036–1038.
- (14) Honeyborne, L. Orange County Health Care Agency, personal communication, 2002.
- (15) Higgins, J. R. *Sampling Theory in Fourier and Signal Analysis*; Oxford University Press: New York, 1996.
- (16) Noble, R. T.; Weisberg, S. B.; Leecaster, M. K.; McGee, C. D.; Ritter, K.; Walker, K. O.; Vainik, P. M. *Environ. Monit. Assess.* 2003, 81, 301–312.
- (17) Taylor, B. N.; Kuyatt, C. E. *Technical Note 1297*; National Institute of Standards and Technology: Gaithersburg, MD, 1994.
- (18) Massey, F. J. *J. Am. Stat. Assoc.* 1951, 46, 68–78.
- (19) Fuhs, G. W. *Sci. Total Environ.* 1975, 4, 165–175.
- (20) Wyer, M. D.; Fleisher, J. M.; Gough, J.; Kay, D.; Merrett, H. *Water Res.* 1995, 29, 1863–1868.
- (21) El-Shaarawi, A. H.; Marsalek, J. *Environmetrics* 1999, 10, 521–529.
- (22) Davies, C. M.; Apte, S. C. *Environ. Toxicol.* 1999, 14, 355–359.
- (23) Heal the Bay (available at <http://www.healthebay.org/brc/>).
- (24) WXTide32 (available at <http://www.wxtide32.com/index.html>).
- (25) Davenport, W. *Probability and Random Processes: An Introduction for Applied Scientists and Engineers*; McGraw-Hill: New York, 1970.
- (26) Turbow, D. J.; Osgood, N. D.; Jiang, S. C. *Environ. Health Perspect.* 2003, 111, 598–603.
- (27) Bowers, J. A.; Shedrow, C. B. *Environ. Stud.* 2000, 4, 89–97.
- (28) Maier, H. R.; Dandy, G. C.; Burch, M. D. *Ecol. Model.* 1998, 105, 257–272.
- (29) Zhang, Q.; Stanley, S. J. *Water Res.* 1997, 31, 2340–2350.

Received for review April 23, 2003. Revised manuscript received November 16, 2003. Accepted November 20, 2003.

ES034382V